

Quantum yields of O(¹D) formation in the photolysis of ozone between 230 and 308 nm

Kenshi Takahashi, Shinsuke Hayashi, and Yutaka Matsumi

Solar-Terrestrial Environment Laboratory and Graduate School of Science, Nagoya University, Aichi, Japan

Nori Taniguchi

Department of Molecular Engineering, Kyoto University, Kyoto, Japan

Sachiko Hayashida

Faculty of Science, Nara Women's University, Nara, Japan

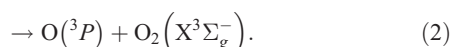
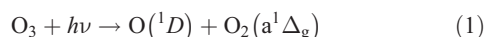
Received 31 December 2001; revised 3 May 2002; accepted 3 May 2002; published 25 October 2002.

[1] Ozone molecules are photolyzed in the strong photoabsorption band of the Hartley band at 230–308 nm, and the O(³P) photofragments produced by the photolysis are detected directly by a technique of laser-induced fluorescence around 130 nm. The quantum yield values for O(¹D) formation in the photolysis of ozone at 297 ± 2 K are determined as a function of the photolysis wavelength, using the O(¹D) quantum yield value of 0.79 at 308 nm as a reference. The O(¹D) quantum yield values obtained are found to be almost independent of the photolysis wavelength over the Hartley band (~0.91). The results are compared with the values measured previously using various experimental techniques and also with the recommendation values for use in atmospheric modeling. The effects of the present yield data on the O(¹D) production rates from ozone photolysis in the stratosphere are evaluated. Impact of our new O(¹D) quantum yield values on the stratospheric chemistry has also been explored using a one-dimensional photochemical model. The smaller O(¹D) production rates as compared to the latest NASA/JPL recommendation values are followed by changes in the efficiency of the chemical chain reactions involving HO_x, NO_x, and ClO_x and result in the higher O₃ concentrations throughout the stratosphere. *INDEX TERMS:* 0317 Atmospheric Composition and Structure: Chemical kinetic and photochemical properties; 0340 Atmospheric Composition and Structure: Middle atmosphere—composition and chemistry; 0365 Atmospheric Composition and Structure: Troposphere—composition and chemistry; *KEYWORDS:* Ozone, oxygen atom, photolysis, quantum yield, ultraviolet, stratosphere

Citation: Takahashi, K., S. Hayashi, Y. Matsumi, N. Taniguchi, and S. Hayashida, Quantum yields of O(¹D) formation in the photolysis of ozone between 230 and 308 nm, *J. Geophys. Res.*, 107(D20), 4440, doi:10.1029/2001JD002048, 2002.

1. Introduction

[2] O₃ plays several extremely important roles in the Earth's atmosphere [Wayne, 2000]. Production of atomic oxygen from the photodissociation of O₃ has been a subject of interest to atmospheric scientists [Ravishankara *et al.*, 1998; Brasseur *et al.*, 1999; Finlayson-Pitts and Pitts, 1999]. Many experimental and theoretical studies have shown that there are two primary pathways in the Hartley band photolysis of O₃ at 220–308 nm;



Both processes are spin-allowed from the singlet state of ozone. Table 1 lists the results from previous measurements of the channel branching ratios between channels (1) and (2) in the Hartley band.

[3] A pioneering study by Fairchild *et al.* [1978] indicated that the formation of O(¹D), channel (1), is dominant over the Hartley band. They photolyzed O₃ molecules at 274 nm and measured the time-of-flight (TOF) spectrum of the fragments. The analysis of the spectrum indicated that the branchings between channels (1) and (2) are ~0.9 and ~0.1, respectively. Sparks *et al.* [1980] also performed experiments at 266 nm using a mass spectrometric detection technique with a molecular beam and reported the channel branching ratio of ~0.1 for the O(³P) formation.

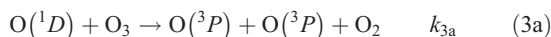
[4] The time-resolved resonance fluorescence detection techniques for O(³P) fragments following O₃ photolysis were also applied to determine the absolute branching ratio between channels (1) and (2) [Amimoto *et al.*, 1980; Brock and Watson, 1980; Wine and Ravishankara, 1982; Green-

Table 1. Summary of O(¹D) Quantum Yield Measurements in the Photolysis of O₃ Between 220 and 300 nm at Room Temperature

λ^a	$\Phi_{1D}(\lambda)^b$	Technique	Note ^c	Reference
222	0.87 ± 0.04	O(³ P) resonance fluorescence	Absolute	Turnipseed et al. [1991]
221–243.5 ^d	0.87–0.88 ^e	O(¹ D) fluorescence	$\Phi_{1D}(248) = 0.91$	Cooper et al [1993]
228.5, 231	0.83 ± 0.04	O(¹ D) fluorescence	$\Phi_{1D}(266) = 0.88$	Cooper et al [1993]
248	0.85 ± 0.02	O(³ P) resonance fluorescence	Absolute	Animoto et al. [1980]
248	0.91 ± 0.03	O(³ P) resonance fluorescence	Absolute	Wine and Ravishankara [1982]
248	0.94 ± 0.01	O(³ P) resonance fluorescence	Absolute	Greenblatt and Weisenfeld [1983]
248	0.91 ± 0.06	O(³ P) resonance fluorescence	Absolute	Talukdar et al. [1997]
253.6	0.92 ± 0.04	decrease in O ₃ pressure	Absolute	Cobos et al. [1983]
266	0.88 ± 0.02	O(³ P) resonance fluorescence	Absolute	Brock and Watson [1980]
266	0.9	time-of-flight mass	Absolute	Sparks et al. [1980]
274	0.9	time-of-flight mass	Absolute	Fairchild et al. [1978]
266–300 ^d	0.85–0.92 ^e	O ₂ (¹ Δ) CARS	Absolute	Valentini et al. [1987]
274–300 ^d	0.86–1.10 ^e	CO ₂ infrared fluorescence	$\Phi_{1D}(308) = 0.79$	Trolier and Wiesenfeld [1988]
297–300 ^d	0.95–1.00 ^e	NO ₂ chemiluminescence	$\Phi_{1D}(300) = 1.00$	Brock and Watson [1980]
270–300 ^d	— ^f	O ₂ (¹ Δ) multiphoton ionization	$\Phi_{1D}(290–300) = 0.95$	Ball et al. [1993]
290–295 ^d	0.90–0.92 ^e	OH laser induced fluorescence	$\Phi_{1D}(308) = 0.79$	Talukdar et al. [1998]
295–300 ^d	0.86–0.91 ^e	NO ₂ chem-ionization mass.	$\Phi_{1D}(308) = 0.79$	Smith et al. [2000]
297–300 ^d	0.88–0.89 ^e	O(³ P) laser induced fluorescence	$\Phi_{1D}(308) = 0.79$	Taniguchi et al. [2000]

^aPhotolysis wavelength in nm.^bO(¹D) quantum yield at the photolysis wavelength λ .^cReference value of $\Phi_{1D}(\lambda)$ at the photolysis wavelength λ is indicated, when a relative method was used in the measurement.^dValues of $\Phi_{1D}(\lambda)$ were measured at a number of points in the wavelength range indicated.^eReported values lie in the range indicated.^fValues of $\Phi_{1D}(\lambda)$ were not presented numerically in the original paper.

blatt and Wiesenfeld, 1983; Turnipseed et al., 1991; Talukdar et al., 1997] at various wavelengths between 222 and 308 nm. Microwave powered oxygen lamps were used to detect the O(³P_j) fragments by either atomic absorption or emission spectroscopy at the resonance line for the 3³S₁–2³P_j transition around 130 nm. In those experiments, time evolutions of the O(³P_j) signal after the laser flash photolysis of O₃ were measured. The time profiles showed a prompt rise due to the direct formation of O(³P) from the photolysis of O₃ in the primary step and a subsequent slow increase as a consequence of the secondary reactions forming O(³P) from O(¹D). The secondary reactions of the O(¹D) atoms with O₃ molecules are



The rate constants of k_{3a} and k_{3b} have been measured to be equal, and the reaction of one O(¹D) with O₃ leads to one O(³P) on the average [DeMore et al., 1997; Talukdar et al., 1997]. Thus the absolute branching ratios were determined by analyzing the time profiles of O(³P) signal intensity, based on the result of $k_{3a}/k_{3b} = 1.0$ in the kinetic studies. Valentini et al. [1987] used coherent anti-Stokes Raman (CARS) spectroscopy to probe the O₂(¹Δ_g) fragments from O₃ photolysis around 280 nm. They determined absolute quantum yields for O₂(¹Δ_g) formation under some assumptions. The O₂(¹Δ_g) quantum yields should reflect the O(¹D) quantum yields, since the dissociation channel (1) is thought to be predominant for O(¹D) formation in the Hartley band photolysis.

[5] Cooper et al. [1993] detected the O(¹D) atoms from the photodissociation of O₃ between 221 and 243.5 nm by observing the weak fluorescence at 630 nm from the spin-forbidden ¹D₂ → ³P transition and measured the relative O(¹D) quantum yields. Ball et al. [1993] used a technique of resonance enhanced multiphoton ionization (REMPI) to detect the O₂(¹Δ_g) fragments and reported the relative

quantum yield for O₂(¹Δ_g) formation between 287 and 329 nm. The detection of O(¹D) using secondary reactions after the photolysis of O₃ at 248 nm was carried out by Talukdar et al. [1998]. They observed the laser-induced fluorescence of OH radicals which were produced by the reaction of the O(¹D) atoms with H₂O or CH₄. They found that the O(¹D) quantum yield is independent of temperature between 200 and 320 K in the photolysis of O₃ at 248 nm.

[6] The NASA/JPL panel has recommended the quantum yield value of 0.95 over the Hartley band between 240 and 300 nm for use in the stratospheric modeling [Sander et al., 2000]. The IUPAC subcommittee [Atkinson et al., 1997] have recommended the formula of (1.98–301/λ) for the photolysis wavelength λ between 271 and 300 nm and a constant value of 0.87 for 222 < λ < 271 nm.

[7] In the present study the O(³P_j) atoms produced in the Hartley band photolysis of O₃ between 230 and 308 nm are directly detected by laser-induced fluorescence in the vacuum UV region (VUV-LIF). Using the VUV-LIF technique, the absolute quantum yields of O(¹D) and O(³P) formation from O₃ photolysis between 297 and 329 nm have been measured previously by our group [Takahashi et al., 1996a; 1996b; 1997; 1998; Taniguchi et al., 2000]. This is the first report on the systematic measurements of the O(¹D) quantum yields from ozone photolysis in the wide range of wavelength in the UV region. As a photolysis light source in this study, an optical parametric oscillator (OPO) with a second harmonic generator, which allowed us to generate tunable UV light in the wide wavelength range, was used. The results obtained in this work were compared with both previously reported values and the recent recommendations for atmospheric modeling by NASA/JPL panel [Sander et al., 2000] and IUPAC subcommittee [Atkinson et al., 1997].

2. Experimental

[8] The experimental arrangement and procedures are essentially the same as in our previous studies on O₃ photolysis [Takahashi et al., 1996a; Taniguchi et al.,

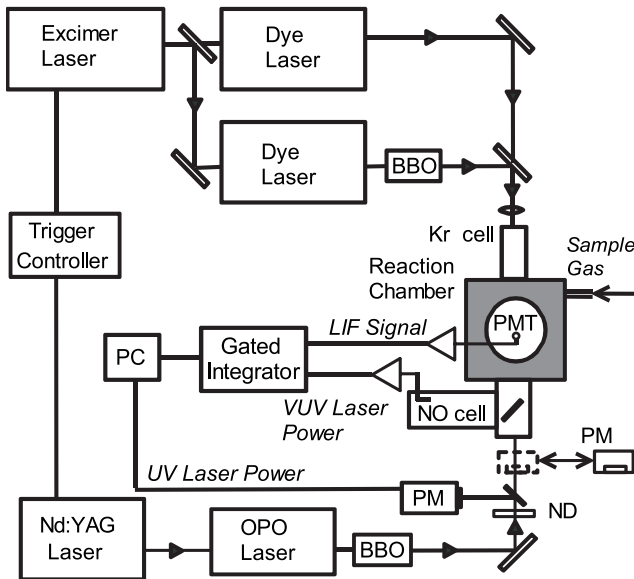


Figure 1. Schematic diagram of experimental setup used in this study. PM: power meter, ND: neutral density optical filter, and PC: personal computer.

2000], except for the photolysis light source. The schematic diagram for the experimental setup is depicted in Figure 1. The O(³P₂) photoproducts were directly detected by the VUV-LIF method using the 3s³S^o-2p³P₂ transition at 130.22 nm. The VUV probe laser was obtained by four-wave mixing in Krypton gas. The output of a XeCl excimer laser (Lambda Physik, LEXtra 50) was split by a dichroic beam splitter (50%/50%) and used to pump simultaneously two tunable dye lasers (Lambda Physik, Scanmate 2 and FL3002). One dye laser operating at 425.12 nm was frequency doubled in β -BaB₂O₄ (BBO) crystal. The UV output was tuned to the wavelength resonant with the two-photon ¹S₀-5p[1/2]₀ transition of Kr at 212.55 nm. The second dye laser was operated at 578.1, 572.8, and 570.6 nm, for detection of three spin-orbit states of $j = 2, 1$, and 0 of O(³P_j), respectively. The two laser beams were mixed using a dichroic beam splitter and focused with a fused silica lens ($f = 200$ mm) into a cell containing 15 Torr of Kr. The resultant VUV light was passed through the MgF₂ window and introduced into the photolysis chamber. A fraction of the VUV light passed through the photolysis chamber was reflected by an MgF₂ beam splitter held in the end of the photolysis chamber and led into a cell containing 3 Torr of nitric oxide (NO). Since the ionization potential of NO is 9.24 eV, the VUV photons at 130 nm ionize NO molecules. The photoionization current from the NO cell was monitored to measure the relative intensity variation of the VUV light. The line width of the VUV laser was about 0.8 cm⁻¹, which was estimated from the line shape of the resonance line of thermalized O(³P_j) atoms.

[9] The photolysis laser light, which was tunable over the range 230–308 nm, was generated using a Nd: YAG laser pumped OPO laser operating at 10 Hz repetition rate (Continuum, Panther OPO and Powerlite 8010), and subsequent frequency doubling using a BBO crystal with an auto-tracking system. The wavelength calibration of the OPO signal light was achieved simultaneously with mea-

urements of the O(³P) spectra by introducing a part of the OPO signal light into a wavemeter (Burleigh, WA-4500). Typical output power of the UV laser light was 1–3 mJ/pulse and the bandwidth was about 6 cm⁻¹(FWHM). A neutral density filter was inserted in the beam path to obtain the appropriate photolysis laser power at various wavelengths. A linear dependence of the O(³P) LIF signal on the UV photolysis laser power was checked at several photolysis wavelengths. The typical results at the photolysis wavelength at 266 nm are shown in Figure 2. During the experiments, the UV laser power was monitored on a shot-by-shot basis using a pyroelectric laser power meter (Molelectron, J4-09). A part of the UV photolysis laser was reflected by a thin fused silica plate onto the power meter. We also monitored the photolysis laser power with a calorimeter (Scientech, AC50UV) by inserting the detector head into the photolysis laser beam path in front of the LIF cell after every LIF measurement. The beam diameter of the photolysis laser was about 5 mm, while that of the probe laser was about 1 mm. The path length of the photolysis laser beam from the inlet to the observation region was about 10 cm.

[10] The photolysis and probe laser beams were counter-propagated and the time delay between the two laser pulses was controlled by a pulse delay controller (Stanford Research, DG535). The delay time was 100 ns with a time jitter less than 5 ns. The LIF of O(³P) was detected along the vertical axis, orthogonal to the propagation direction of both VUV probe and photolysis laser beams, using a solar-blind photomultiplier tube (PMT) (EMR, 541J-08-17). The PMT has a LiF window and a KBr photocathode that is sensitive only between 105 and 150 nm. The output from the PMT was preamplified and fed into a gated integrator (Stanford Research, SR-250).

[11] The reaction chamber was evacuated by a rotary pump (330 Liter/min). The ozone gas was synthesized from

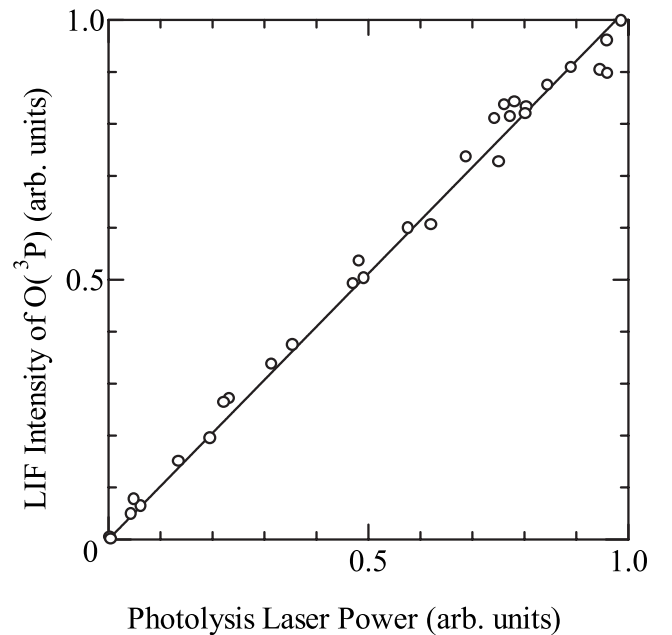


Figure 2. Photolysis laser power dependence of the laser-induced fluorescence intensity for the O(¹D) atoms in the ozone photolysis at 266 nm. A straight line indicates the result of linear least squares fit analysis.

ultrapure O₂ (Nagoya Kosan, 99.9995%) by a silent discharge ozonizer. The O₃ gas was flowed slowly into the reaction chamber through a polytetrafluoroethylene tube. Helium gas was added as a buffer gas. The total pressure in the reaction cell was maintained to be 1.5 Torr. The partial pressure of O₃/O₂ was 0.35 Torr and which of about 3% was O₃. The pressure was measured with a capacitance manometer (MKS, Baratron, 2 Torr full scale). It should be noted that the high sensitivity of the VUV-LIF technique makes it possible to detect O(³P_j) atoms at such low pressure and short pump-probe delay time, and that secondary reactions can be safely ignored. For example, the rate constant for the reaction O(¹D) + O₂(X³Σ_g⁻) is reported to be 4×10^{-11} cm³ molecule⁻¹ s⁻¹ and that of O(¹D) + O₃ to form 2O(³P) is 1.2×10^{-10} cm³ molecule⁻¹ s⁻¹ at 298 K [Sander *et al.*, 2000]. Helium used as the buffer gas is inefficient quencher for O(¹D), that is, the rate constant is $< 5 \times 10^{-14}$ cm³ molecule⁻¹ s⁻¹ at 298 K [Stief *et al.*, 1975]. We estimated that the formation of O(³P_j) atoms through these reactions from O(¹D) is less than 0.5% under our experimental conditions. All experiments in the present study were performed at room temperature (297 ± 2 K).

3. Results

[12] Figure 3 shows a typical example of the O(³P) quantum yield measurements, in which O₃ molecules were photolyzed by UV laser pulses at 308 and 266 nm alternatively, and the O(³P₂) photofragments were probed directly by the VUV-LIF method. The detection wavelength for O(³P₂) atoms was fixed at 130.22 nm, which was the peak wavelength of the electronic transition of 3s²S^o-2p³P₂. The absolute quantum yield of 0.79 for O(¹D), that is, the yield of 0.21 for O(³P) at the photolysis wavelength of 308 nm was used as the reference value to obtain the yields at the wavelengths between 230 and 308 nm. The yield value of 0.79 at 308 nm is based on the recent review paper [Matsumi *et al.*, 2001] that recommended the quantum yield values for O(¹D) formation in the photodissociation of O₃ as a function of the wavelength and temperature for use in atmospheric modeling. In the yield measurements, the wavelength of the photolysis laser was changed alternatively between the reference (308 nm) and target wavelengths, as shown in Figure 3. From the comparison of signal intensities at the two photolysis wavelengths, we obtained the quantum yield values for O(³P) formation in the photodissociation of O₃, using the following expression:

$$\Phi_{3P}(\lambda) = \Phi_{3P}(308) \times \frac{S(\lambda)}{S(308)} \frac{I(308)}{I(\lambda)} \frac{\sigma(308)}{\sigma(\lambda)}, \quad (4)$$

where $\Phi_{3P}(\lambda)$ is the O(³P) quantum yield at a photolysis wavelength λ , S(λ) is the LIF intensity which is corrected by intensity variation of the VUV probe laser, I(λ) is the photon flux of the UV photolysis laser, $\sigma(\lambda)$ is the O₃ absorption cross section reported by Malicet *et al.* [1995], and $\Phi_{3P}(308)$ is the quantum yield for O(³P) formation at 308 nm (0.21). The O(¹D) quantum yield as a function of wavelength is given by:

$$\Phi_{1D}(\lambda) = 1 - \Phi_{3P}(\lambda). \quad (5)$$

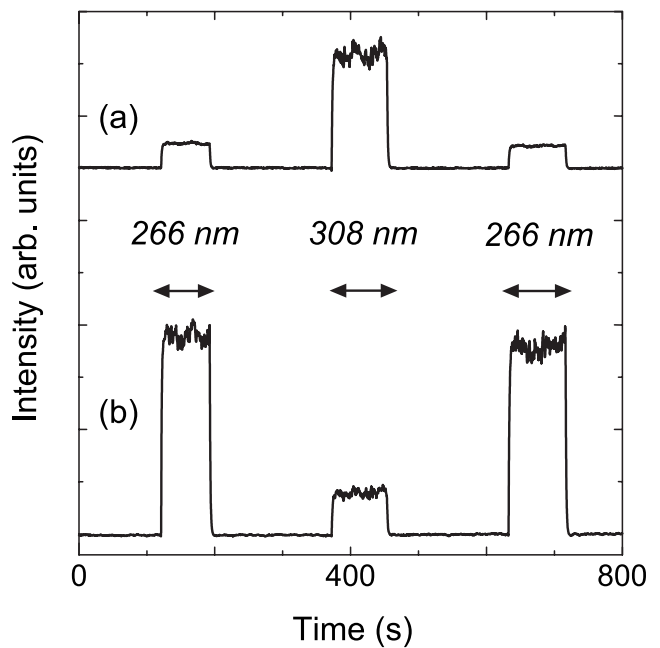
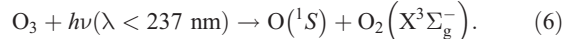


Figure 3. Typical experimental results for the O(³P) quantum yield measurements in the photolysis of O₃ at 297 ± 2 K. (a) Laser-induced fluorescence intensity of O(³P₂) atoms at 266 and 308 nm. (b) Photolysis laser power at 266 and 308 nm. Arrows indicate the time periods in which the photolysis laser is introduced into the reaction chamber and the LIF signal is detected.

At the photolysis wavelengths shorter than 237 nm, the formation of O(¹S) is energetically possible [Okabe, 1978]:



However, the dissociation process (6) is spin-forbidden and the upper limit for the O(¹S) quantum yield has been reported to be 0.1% between 170 and 240 nm [Lee *et al.*, 1980]. It is thus reasonable to ignore the contribution of the process (6) between 230 and 237 nm.

[13] Figure 3 shows the signal intensities of O(³P_j, j = 2) produced from the photolysis of ozone at 266 and 308 nm in the VUV-LIF spectroscopy. The photodissociation process (2) produces not only the j = 2 spin-orbit state of O(³P_j) but also j = 1 and 0 states. Under our experimental conditions that the total pressure is 1.5 Torr and the delay time is 100 ns, the j-populations are partly relaxed toward the Boltzmann distribution [Abe *et al.*, 1994]. We measured the relative j-populations among the O(³P_j) j = 2, 1, and 0 states from ozone photolysis at several wavelengths in the range of 230–308 nm under the same experimental conditions as the quantum yield measurements. The relative j-populations obtained in this study are summarized in Table 2. There is no remarkable dependence on the photolysis wavelength in the spin-orbit populations within the experimental errors in this wavelength range. This indicates that the relative signal intensities of the j = 2 can be used in the calculations of the total O(³P_j) formation yield in equation (4).

[14] The signal intensities shown in Figure 3 were measured when the probe VUV laser wavelength was fixed at the peak of the O(3s²S^o-2p³P₂) transition. If the line width of the

Table 2. Relative Populations Among the Three Spin-Orbit States of O(³P_j) Produced in the Ultraviolet Photolysis of O₃ Between 230 and 308 nm Under Our Experimental Conditions

Photolysis Wavelength, nm	O(³ P _j)		
	j = 2	j = 1	j = 0
238	0.64 ± 0.03	0.28 ± 0.02	0.08 ± 0.01
263	0.66 ± 0.04	0.27 ± 0.03	0.07 ± 0.01
287	0.65 ± 0.03	0.25 ± 0.03	0.10 ± 0.02

spectral shape for the O(³P₂) fragments due to the Doppler broadening were strongly dependent on the photolysis wavelength, the intensities of the O(³P₂) fragments at the peaks might not be proportional to the total O(³P) yields. We measured the line profiles of nascent O(³P) atoms at various photolysis wavelengths between 230 and 308 nm by scanning the wavelength of the VUV probe laser (band width ≈ 0.8 cm⁻¹) around the resonance center of 3s³S°–2p³P₂ transition. No obvious variation in the spectral shape was observed.

[15] The O(¹D) quantum yields thus obtained in the wavelength range of 230–308 nm are shown in Figure 4. For comparison, the O(¹D) quantum yields reported by other groups are also shown in Figure 4. Table 3 lists the O(¹D) quantum yield values obtained in this work. Quoted errors indicate the two standard deviations (2σ) of the measurements, which are due to the standard deviations associated with the 5–10 times experimental measurements of LIF signal intensities of O(³P_j) and the uncertainties in photolysis laser power measurements with a laser power meter. It should be noted that the previous studies on the quantum yield measurements in the Hartley band were carried out mostly around 290 nm. The small number of measurements in the shorter wavelengths may be due to the difficulty to obtain the photolysis light source that can cover the wide wavelength range over the Hartley band of O₃. In our present study, we employed the tunable OPO laser

Table 3. The Quantum Yield Values of O(¹D) Formation in the Hartley Band Photolysis of O₃ at 297 ± 2 K as a Function of Photolysis Wavelength λ in nm.

λ	Φ _{1D} (λ)	Uncertainty (2σ)
230	0.910	0.019
232	0.917	0.017
234	0.928	0.016
236	0.906	0.022
238	0.908	0.019
240	0.910	0.020
242	0.885	0.025
244	0.899	0.022
246	0.896	0.023
248	0.914	0.019
250	0.900	0.021
252	0.914	0.019
254	0.921	0.016
256	0.916	0.018
258	0.914	0.020
260	0.905	0.020
261.5	0.915	0.019
262.5	0.910	0.019
266	0.919	0.017
267.2	0.926	0.020
267.5	0.927	0.016
269	0.922	0.017
269.8	0.924	0.016
270	0.924	0.017
272	0.923	0.017
274	0.908	0.022
276	0.900	0.023
278	0.894	0.025
280	0.891	0.032
284	0.873	0.021
288	0.879	0.011
292	0.892	0.018
296	0.881	0.022

pumped by the third harmonics of the Nd:YAG laser for the photolysis light source. It could cover the whole wavelength range of our interest in the present study without any realignment of the laser system. The usage of the combination of a tunable dye laser and a nonlinear crystal for UV generation requires frequent changes of dye solutions and crystals to cover the entire range of the Hartley band, which consequently reduces the accuracies in the measurements of the O(¹D) quantum yield in the wide wavelength range.

4. Discussion

4.1. Quantum Yield for O(¹D) Formation in the Hartley Band Photolysis of O₃

[16] We have measured the wavelength dependence of the O(¹D) quantum yield from O₃ photolysis at 2-nm intervals between 230 and 308 nm. As shown in Figure 4, it has been found that the values obtained in this work are almost independent of the photolysis wavelengths (≈ 0.91). At 248 nm which is the center of the strong absorption of the Hartley band, the room temperature O(¹D) quantum yield was reported to be 0.91 ± 0.06 by Talukdar et al. [1997] and 0.94 ± 0.01 by Greenblatt and Wiesenfeld [1983]. Our measured value of Φ_{1D}(248) = 0.914 ± 0.019 is in good agreement with their results. Taniguchi et al. [2000] measured the photofragment excitation spectrum for O(³P) from O₃ photolysis in the wavelength range of 296–314 nm and obtained the O(¹D) quantum yield values. Talukdar et al. [1998] reported that the O(¹D) quantum yield between 289

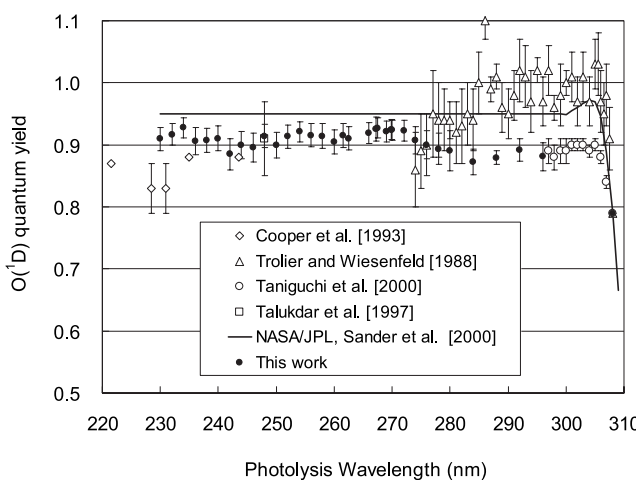


Figure 4. The quantum yield for O(¹D) formation in the Hartley band photolysis of O₃ at 297 ± 2 K as a function of photolysis wavelength. For comparison, the yield values reported by other groups are also shown. A solid curve indicates the yield values recommended by NASA/JPL panel [Sander et al., 2000], which are constant (0.95) between 240 and 300 nm.

and 305 nm was 0.89 ± 0.02 . The present results are in good agreement with their results. It has also been shown that the results presented by *Trolier and Wiesenfeld* [1988] are larger than those obtained in this work and also than the results of recent studies by *Talukdar et al.* [1998] and *Taniguchi et al.* [2000]. Since the O(¹D) quantum yields at some wavelengths reported by *Trolier and Wiesenfeld* [1988] exceed 1 between 285 and 306 nm, they may overestimate the quantum yields of O(¹D) in this wavelength region. *Cooper et al.* [1993] observed weak 630-nm fluorescence from the spin-forbidden O(¹D) \rightarrow O(³P) transition in the photolysis of O₃ between 221 and 243.5 nm and determined the O(¹D) quantum yields. They indicated the O(¹D) quantum yield was almost constant in this wavelength range. Their values are close to those obtained in this study, except for 231 nm.

[17] The NASA/JPL panel recommends the constant value of 0.95 as the quantum yield for O(¹D) formation in the Hartley band photolysis of O₃ between 240 and 300 nm for use in atmospheric modeling [*Sander et al.*, 2000]. For $222 < \lambda < 271$ nm, the IUPAC subcommittee [*Atkinson et al.*, 1997] have recommended a constant value (0.87) which is a little smaller than the values obtained in this study, while they recommended larger values than ours near 300 nm.

[18] The Hartley band has been assigned to the strongly allowed ¹B₂-¹A₁ transition [*Hay et al.*, 1982]. Photoexcitation to the repulsive limb of the excited ¹B₂ state results in prompt dissociation into O(¹D) + O₂(¹Δ_g) products (channel (1)). Surface crossing from the initially prepared ¹B₂ state to a repulsive (*R*) state provides O(³P) + O₂(X³Σ_g⁻) products (channel (2)). Our experimental results show that the channel branching ratio between O(¹D) and O(³P) formation does not strongly depend on the photolysis wavelength over the Hartley band (Figure 4 and Table 3). This suggests that the efficiency of the potential switching from the ¹B₂ state to the *R* state is almost independent of the excitation energy.

4.2. Atmospheric Implications

[19] Chemical reactions of the O(¹D) atoms with trace gas molecules are key processes to determine the chemical nature of the Earth's atmosphere. For instance, the reactions of O(¹D) + N₂O and O(¹D) + H₂O are the direct source for stratospheric NO_x and HO_x molecules. The atmospheric production rates of O(¹D) atom from O₃ photolysis at several altitudes, P_{total}(O¹D), were calculated using the quantum yield values for O(¹D) formation measured in this study.

$$P_{\text{total}}(\text{O}^1\text{D}) = \int P(\lambda)d\lambda = \int F(\lambda)\sigma(\lambda)\Phi_{1\text{D}}(\lambda)d\lambda \quad (7)$$

In the equation (7), F(λ) is the altitude dependent solar photon flux as a function of λ. The calculations were performed for the altitudes of 15, 25, and 40 km. The solar zenith angle was fixed at 40 degree. The numerical data of the solar photon flux were taken from *Finlayson-Pitts and Pitts* [1999]. The absorption cross sections of O₃ were taken from *Malicet et al.* [1995].

[20] In the calculations, for the wavelengths longer than 300 nm, the expression for the O(¹D) quantum yield recommended by NASA/JPL [*Sander et al.*, 2000] was used, which is functions of photolysis wavelength and temperature. At $\lambda > 300$ nm, the photodissociation of the vibrationally and rotationally excited O₃ takes place. Even at longer wavelengths

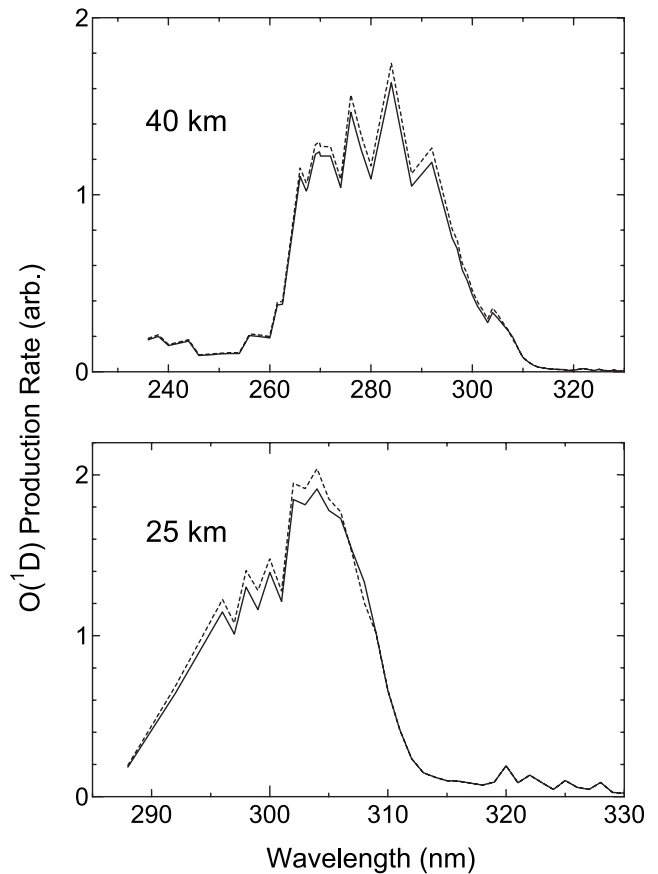
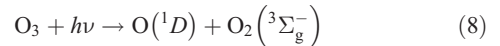


Figure 5. Production rates of O(¹D) produced from the photolysis of O₃ as functions of solar wavelength in the stratosphere at altitudes of 25 and 40 km. Solid curves indicate the results based on the O(¹D) quantum yield values obtained in this work, while broken ones are the results based on the NASA/JPL recommendations [*Sander et al.*, 2000].

than the channel (1) threshold (≈ 310 nm) O(¹D) atoms are produced [*Ravishankara et al.*, 1998; *Takahashi et al.*, 1998]. Since the population of the internally excited O₃ molecules is dependent on the temperature, the O(¹D) quantum yield at $\lambda > 305$ nm changes as a function of the temperature. The O(¹D) formation via the following spin-forbidden process takes place at $\lambda > 310$ nm [*Ravishankara et al.*, 1998; *Takahashi et al.*, 1998]:



[21] It is assumed that the O(¹D) quantum yield in the Hartley band at $\lambda < 300$ nm has no temperature dependence. The recent experimental study at 248 nm showed no temperature dependence of the O(¹D) quantum yield [*Talukdar et al.*, 1997]. At 305 nm, *Takahashi et al.* [1998] showed that the O(¹D) quantum yield has a negligible temperature dependence. *Talukdar et al.* [1998] also reported that the O(¹D) quantum yield between 289 and 305 nm was independent of the temperature (203–320 K).

[22] Figure 5 shows the relative O(¹D) production rate functions P(λ) in the stratosphere at the altitudes of 25 and

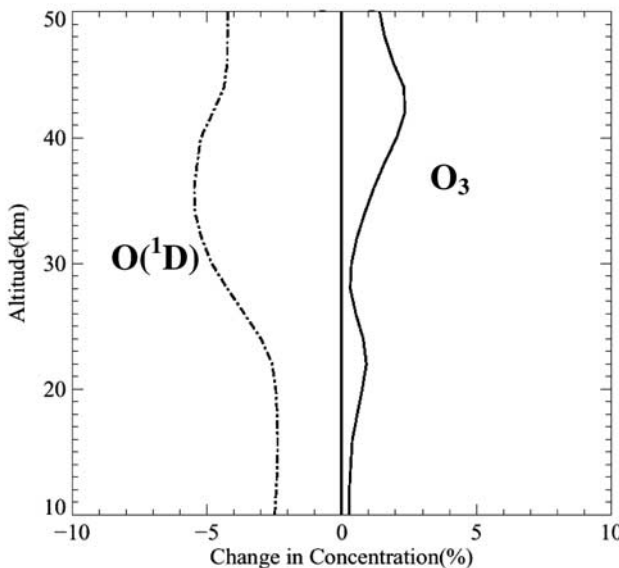


Figure 6. Calculated percentage change in O(¹D) and O₃ concentrations for latitude of 40 degree in March as a function of altitude using the new O(¹D) quantum yield values measured in this study, relative to the NASA/JPL recommendations [Sander et al., 2000].

40 km, using the (¹D) quantum yield values obtained in this study and those recommended by NASA/JPL [Sander et al. 2000]. The total O(¹D) production rates P_{total}(O(¹D)) calculated with our O(¹D) quantum yield data are smaller than those with the NASA/JPL recommendation by 1.7, 3.3 and 5.0%, at 15, 25 and 40 km, respectively.

[23] In this study, we have examined the effect of our O(¹D) quantum yield values using a one-dimensional dynamical-photochemical model, in which all the chemical reactions related to ozone chemistry are reasonably represented and it is suitable for assessing the impact of our new O(¹D) quantum yield data on stratospheric chemistry. All chemical schemes are the same with that in the Garcia-Solomon two-dimensional (GS-2D) model [e.g., Solomon et al., 1996]. In this study, the model calculations were performed including 40 chemical species and 120 chemical reactions with the chemical kinetics and photochemical data presented by the recent JPL recommendations [DeMore et al., 1997; Sander et al., 2000].

[24] Figure 6 shows the result of the photochemical model calculations, which indicates the change of the O(¹D) and O₃ concentrations for latitude of 40 degree in March between the model runs with our new O(¹D) values and the NASA/JPL recommendations. The steady state O(¹D) concentration becomes smaller by 2–6% depending on altitude in the stratosphere. This result is consistent with our evaluation of the altitudinal changes in the O(¹D) production rate as shown in Figure 5. The O₃ concentration evaluated with our O(¹D) yield is higher than that done with the NASA/JPL recommendation throughout the stratosphere as shown in Figure 6. This is due to the changes in the efficiency of the chain reactions involving HO_x, NO_x, and ClO_x families through the lower O(¹D) production rate. Our study may contribute to precise assessment of the photochemical O₃ budget including the “ozone deficit” problem [Crutzen, 1997] that

implies a number of model calculations underestimate the O₃ concentrations in the upper stratosphere and mesosphere.

5. Conclusion

[25] The quantum yield value of the O(¹D) formation in the Hartley band photolysis of O₃ has been examined as a function of the wavelength, using the laser flash photolysis technique with the laser-induced fluorescence detection of the atomic oxygen fragments. The detailed measurements by 2-nm interval have been performed for the wide wavelength range of the Hartley band. The measured quantum yield was almost independent of the photolysis wavelength between 230 and 305 nm, with the almost constant value of 0.88–0.93. The results were compared with the previously reported values and the latest NASA/JPL and IUPAC recommendation for atmospheric modeling. The relative production rates of O(¹D) from O₃ photolysis in the stratosphere have been evaluated. We have shown that the atmospheric O(¹D) production rates calculated with the O(¹D) quantum yield values obtained in this study are smaller than those calculated with the latest NASA/JPL recommendation by 1.7, 3.3 and 5.0%, at the altitudes of 15, 25 and 40 km, respectively. Using the one-dimensional photochemical model, change of the O₃ concentration between the runs with our new O(¹D) yield values and the NASA/JPL recommendations has also been examined. The smaller O(¹D) production rates are followed by changes in the efficiency of the chemical chain reactions involving HO_x, NO_x, and ClO_x, and result in the higher O₃ concentrations throughout the stratosphere.

[26] **Acknowledgments.** This work was supported by a Grant-in-Aid from the Ministry of Education, Culture, Sports, Science and Technology, Japan. N. T. thanks the Japan Society for Promotion of Science for a fellowship for young scientists. The one-dimensional model used in this study was originally offered by Susan Solomon, NOAA Aeronomy Laboratory. The authors are grateful to Yukari Shibata and Nao Ikeda for their help on the model calculations.

References

- Abe, M., Y. Sato, Y. Inagaki, Y. Matsumi, and M. Kawasaki, Collisional relaxation of translational energy and fine-structure levels of the O(³P_j) atom created in the photodissociation of SO₂ at 193 nm, *J. Chem. Phys.*, 101, 5647–5651, 1994.
- Amimoto, S. T., A. P. Force, J. R. Wiesenfeld, and R. H. Young, Direct observation of O(³P_j) in the photolysis of O₃ at 248 nm, *J. Chem. Phys.*, 73, 1244–1247, 1980.
- Atkinson, R., D. L. Baulch, R. A. Cox, R. F. Hampson Jr, J. A. Kerr, M. J. Rossi, and J. Troe, Evaluated kinetic and photochemical data for atmospheric chemistry: Supplement VI, *J. Phys. Chem. Ref.*, 1329–1499, 1997.
- Ball, S. M., G. Hancock, I. J. Murphy, and S. P. Rayner, The relative quantum yield of O₂(¹Δ_g) from the photolysis of ozone in the wavelength range 270 nm < λ < 329 nm, *Geophys. Res. Lett.*, 20, 2063–2066, 1993.
- Brasseur, G. P., J. J. Orlando, and G. S. Tyndall, *Atmospheric Chemistry and Global Change*, Oxford Univ. Press, New York, 1999.
- Brock, J. C., and R. T. Watson, Ozone photolysis: Determination of O(³P) quantum yield at 266 nm, *Chem. Phys. Lett.*, 71, 371–375, 1980.
- Cooper, I. A., P. J. Neill, and J. R. Wiesenfeld, Relative quantum yield of O(¹D₂) following ozone photolysis between 221 and 243.5 nm, *J. Geophys. Res.*, 98, 12,795–12,800, 1993.
- Crutzen, P. J., Mesospheric mysteries, *Science*, 277, 151–152, 1997.
- DeMore, W. P., S. P. Sander, C. J. Howard, A. R. Ravishankara, D. M. Golden, C. E. Kolb, R. F. Hampson, M. J. Kurylo, and M. J. Molina, Chemical kinetics and photochemical data for use in stratospheric modeling, *JPL Publ.*, 97-4, Eval. 12, Jet Propul. Lab., Pasadena, Calif., 1997.

- Fairchild, C. E., E. J. Stone, and G. M. Lawrence, Photofragment spectroscopy of ozone in the uv region 270–310 nm and at 600 nm, *J. Chem. Phys.*, **69**, 3632–3638, 1978.
- Finlayson-Pitts, B. J., and J. N. Pitts Jr., *Chemistry of the Upper and Lower Atmosphere: Theory, Experiments, and Applications*, Academic, San Diego, Calif., 1999.
- Greenblatt, G. D., and J. R. Wiesenfeld, Time-resolved fluorescence studies of O(¹D₂) yields in the photodissociation of O₃ at 248 and 308 nm, *J. Chem. Phys.*, **78**, 4924–4928, 1983.
- Hay, P. J., R. T. Pack, R. B. Walker, and E. J. Heller, Photodissociation of ozone in the Hartley band: Exploratory potential energy surfaces and molecular dynamics, *J. Phys. Chem.*, **86**, 862–865, 1982.
- Lee, L. C., G. Black, R. L. Sharpless, and T. G. Slanger, O(¹S) yield from O₃ photodissociation at 1700–2400 Å, *J. Chem. Phys.*, **73**, 256–258, 1980.
- Malicet, J., D. Daumont, J. Charbonnier, C. Parisse, A. Chakir, and J. Brion, Ozone UV spectroscopy, II, Absorption cross-sections and temperature dependence, *J. Atmos. Chem.*, **21**, 263–273, 1995.
- Matsumi, Y., F. J. Comes, G. Hancock, A. Hofzumahaus, A. J. Hynes, M. Kawasaki, and A. R. Ravishankara, Quantum yields for production of O(¹D) in the ultraviolet photolysis of ozone: Recommendation based on evaluation of laboratory data, *J. Geophys. Res.*, **107(D3)**, 4024, doi:10.1029/2001JD000510, 2002.
- Okabe, H., *Photochemistry of Small Molecules*, Wiley-Interscience, New York, 1978.
- Ravishankara, A. R., G. Hancock, M. Kawasaki, and Y. Matsumi, Photochemistry of Ozone: Surprises and Recent Lessons, *Science*, **280**, 60–61, 1998.
- Sander, S. P., R. R. Friedel, R. E. Huie, M. J. Kurylo, C. E. Kolb, D.M. Golden, A. R. Ravishankara, and M. J. Molina, *Chemical Kinetics and Photochemical Data for Stratospheric Modeling*, JPL Publ. 00-3, JPL, Pasadena, Calif., 2000.
- Solomon, S., R. W. Portmann, R. R. Garcia, L. W. Thomason, L. R. Poole, and M. P. McCormick, The role of aerosol variations in anthropogenic ozone depletion at northern midlatitudes, *J. Geophys. Res.*, **101**, 6713–6727, 1996.
- Sparks, R. K., L. R. Carlson, K. Shobatake, M. L. Kowalczyk, and Y. T. Lee, Ozone photolysis: A determination of the electronic and vibrational state distributions of primary products, *J. Chem. Phys.*, **72**, 1401–1402, 1980.
- Stief, L. J., W. A. Payne, and R. B. Klemm, A flash photolysis-resonance fluorescence study of the formation of O(¹D) in the photolysis of water and the reaction of O(¹D) with H₂, Ar, and He, *J. Chem. Phys.*, **62**, 4000–4008, 1975.
- Takahashi, K., Y. Matsumi, and M. Kawasaki, Photodissociation processes of ozone in the Huggins band at 308–326 nm, *J. Chem. Phys.*, **100**, 4084–4089, 1996a.
- Takahashi, K., M. Kishigami, Y. Matsumi, M. Kawasaki, and A. J. Orr-Ewing, Observation of the spin-forbidden O(¹D) + O₂(X³Σ_g⁻) channel in the 317–327 nm photolysis of ozone, *J. Chem. Phys.*, **105**, 5290–5293, 1996b.
- Takahashi, K., M. Kishigami, N. Taniguchi, Y. Matsumi, and M. Kawasaki, Photofragment excitation spectrum for O(¹D) from the photodissociation of jet-cooled ozone in the wavelength range 305–329 nm, *J. Chem. Phys.*, **106**, 6390–6397, 1997.
- Takahashi, K., N. Taniguchi, Y. Matsumi, M. Kawasaki, and M. N. R. Ashfold, Wavelength and temperature dependence of the absolute O(¹D) production yield from the 305–329 nm photodissociation of ozone, *J. Chem. Phys.*, **108**, 7161–7172, 1998.
- Talukdar, R. K., M. K. Gilles, F. Battin-Leclerc, A. R. Ravishankara, J.-M. Fracheboud, J. J. Orlando, and G. S. Tyndall, Photolysis of ozone at 308 and 248 nm: Quantum yield of O(¹D) as a function of temperature, *Geophys. Res. Lett.*, **24**, 1091–1094, 1997.
- Talukdar, R. K., C. A. Langfellow, M. K. Gilles, and A. R. Ravishankara, Quantum yields of O(¹D) in the photolysis of ozone between 289 and 329 nm as a function of temperature, *Geophys. Res. Lett.*, **25**, 143–146, 1998.
- Taniguchi, N., K. Takahashi, and Y. Matsumi, Photodissociation of O₃ around 309 nm, *J. Phys. Chem.*, **A104**, 8936–8944, 2000.
- Trolier, M., and J. R. Wiesenfeld, Relative quantum yield of O(¹D₂) following ozone photolysis between 275 and 325 nm, *J. Geophys. Res.*, **93**, 7119–7124, 1988.
- Turnipseed, A. A., G. L. Vaghjiani, T. Gierczak, J. E. Thompson, and A. R. Ravishankara, The photochemistry of ozone at 193 nm and 222 nm, *J. Chem. Phys.*, **95**, 3244–3251, 1991.
- Valentini, J. J., D. R. Gerry, D. L. Phillips, J.-C. Nieh, and K. D. Tabor, CARS spectroscopy of O₂(¹Δ_g) from the Hartley band photodissociation of O₃: Dynamics of the dissociation, *J. Chem. Phys.*, **86**, 6745–6756, 1987.
- Wayne, R. P., *Chemistry of Atmospheres*, 3rd edition, Oxford Univ. Press, New York, 2000.
- Wine, P. H., and A. R. Ravishankara, O₃ photolysis at 248 nm and O(¹D₂) quenching by H₂O, CH₄, H₂, and N₂O: O(³P_j) yields, *Chem. Phys.*, **69**, 365–373, 1982.

S. Hayashi, Y. Matsumi, and K. Takahashi, Solar-Terrestrial Environment Laboratory and Graduate School of Science, Nagoya University, Honohara 3-13, Toyokawa, Aichi, 442-8507, Japan. (matsumi@stelab.nagoya-u.ac.jp; kent@stelab.nagoya-u.ac.jp)

S. Hayashida, Faculty of Science, Nara Women's University, Kita-uoya Nishi-machi, Nara, 630-8506, Japan. (sachiko@ics.nara-wu.ac.jp)

N. Taniguchi, Department of Molecular Engineering, Kyoto University, Yoshidahonmachi, Sakyou-ku, Kyoto, 606-8501, Japan. (ntanig@jp.media.kyoto-u.ac.jp)